ELSEVIER

Nuclear Engineering and Design 215 (2002) 199–216

Nuclear Engineering and Design

www.elsevier.com/locate/nucengdes

A study of the performance of void fraction correlations used in the context of drift-flux two-phase flow models

Paul Coddington *, Rafael Macian

Laboratory for Reactor Physics and Systems Behavior, Paul Scherrer Institute, CH-5232 Villigen PSI, Switzerland

Received 16 February 2001; received in revised form 20 April 2001; accepted 31 October 2001

Abstract

Drift-flux models have traditionally been and are currently used in thermal-hydraulic analysis codes in the nuclear and other industries to analyze the behavior of systems during a wide variety of transient conditions. Their simplicity and closeness to experimental data, compared to two-fluid models, and their robustness, make them a cost-effective and efficient choice, although these models are generally limited to co-current flow. The drift-flux models are based on correlations to compute the void fraction distribution and slip in two-phase flow needed to obtain the relative velocity between the phases. Thus, the accuracy of the correlations has a decisive role in determining the correct transport of vapor along the system and, subsequently, in the prediction of the correct response of nuclear or industrial systems. This paper presents the results of an evaluation of the accuracy of a range of widely used void fraction correlations based on the Findlay–Zuber drift-flux model. The 13 correlations presented in this paper, a sub-set of all considered, can loosely be termed as 'wide range void correlations', since, as shown in this paper, they are those able to perform reasonably well for the wide range of experimental conditions used in the assessment. The size of the experimental database allowed a detailed statistically based comparison of the performance of all the correlations assessed. The void fraction data is taken from rod bundle, level swell and boil-off experiments performed within the last 10–15 years at 9 experimental facilities in France, Japan, Switzerland, the UK and the USA. The pressure and mass fluxes of the analyzed experiments range from 0.1 to 15 MPa and from 1 to 2000 kg m^{-2} s^{-1}, respectively. Finally, the assessment of a widely used correlation against experimental transient void fraction data has been performed. The selected correlation is that of Chexal–Lellouche, currently used in the system codes RETRAN-3D and RELAP-5. The results show the performance of the correlation when used in the context of a system code and two different drift-flux model approaches, namely, an algebraic slip calculation and the calculation of the slip velocity based on the solution of a differential slip equation. The accuracy of the predictions shows that it is possible to use a drift-flux approach even for the analysis of rapid transients.

1. Introduction

Thermal-hydraulic analysis codes solve the mass, momentum and energy conservation equations with the help of closure relationships. In these codes, void fraction prediction is a function

* Corresponding author.
E-mail addresses: paul.coddington@psi.ch (P. Coddington), rafael.macian@psi.ch (R. Macian).

0029-5493/02/$ - see front matter
PII: S0029-5493(01)00503-9

of energy transfer to the fluid and of transport of the vapor phase along the system. Models to predict the boiling and relative velocity between the phases are thus necessary. Such models are often based on correlations containing empirically derived constants due to the lack of theoretical knowledge or to the complexity of the physical processes involved. One of the models used to calculate void fraction is the drift-flux model of Zuber and Findlay (Zuber and Findlay, 1965). It provides the starting point for most of the void correlations reviewed in this paper.

In the drift-flux model, the void fraction α is a function of the total and vapor superficial velocities, j and j_g, a phase distribution parameter C_0 and a drift velocity v_{gj}. In this form, vapor production, computed from a boiling model, is included in j_g, and the effect of the relative velocity between the phases is included in v_{gj}.

$$\alpha = \frac{j_g}{C_0 j + v_{gj}} \tag{1}$$

In general, drift-flux correlations offer procedures to compute C_0 and v_{gj}. Assessment of the predictions of α by the correlations against data from a wide range of experimental facilities at various pressures and mass fluxes provides the opportunity to determine their overall applicability.

2. Experimental rod bundle void fraction data

A wide range of rod bundle experimental void fraction data has been collected. The data covers pressures from 0.1 to 15 MPa and mass fluxes from 1 to 2000 kg m^{-2} s^{-1}, and so provides information on void fractions in rod bundles (reactor cores) including BWR normal operating conditions, and small and large break transient conditions for both PWRs and BWRs. The majority of this data is from steady state or quasi steady state (slow boil-down) experiments. The current data base includes 362 individual data points.

The experimental data collected comes from recent rod bundle void fraction measurements taken from test facilities in France (PERICLES), Japan (BWR 4×4, BWR 8×8, LSTF, TPTF), Switzerland (NEPTUN), the UK (ACHILLES, THETIS) and the USA (THTF). A detailed list of the experimental facilities and selected parameters is given in Table 1. Fig. 1 provides an indication of the wide range of pressures and mass fluxes covered by the experimental data. The void fraction data is based on pressure drop measurements, unless otherwise mentioned.

3. Void fraction correlations and results

The experimental data has been used to assess the predictive capability of the correlations used in several widely used thermal-hydraulic analysis codes. A literature search produced over 25 different void correlations published between 1965 and 1995, many of which were limited in their range of application to conditions similar to those from which they were derived. Of them, 13 correlations produced 'acceptable' results over the whole range of data.

In order to determine the quality of the predictions the absolute error for each data point was calculated as

$$\varepsilon = \alpha_{meas} - \alpha_{pred} \tag{2}$$

The mean absolute error and the standard deviation of the absolute error were then used to compare the correlations,

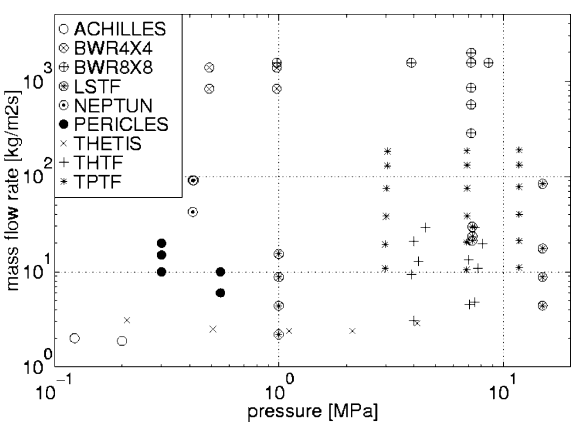

Fig. 1. Pressures and mass fluxes of the experimental data.

Table 1
Overview of the experimental facilities and the significant parameters (sorted by pressure)

	ACHILLES	THETIS	PERICLES	NEPTUN	BWR 4×4	BWR 8×8	LSTF	TPTF	THTF
Reference	Pearson and Denham, 1989	Jowitt et al., 1984	Deruaz et al., 1985	Dreier et al., 1988	Mitsutake et al., 1990	Morooka et al., 1991	Anoda et al., 1990	Kumamaru et al., 1994	Anklam and Miller, 1982
Type	PWR	BWR	PWR	LWHCR[a]	BWR	BWR	PWR	PWR	PWR
Length [m]	3.7	3.6	3.7	1.7	3.7	3.7	3.7	3.7	3.7
Rods (heated)	69(69)	49(49)	357(357)	37(37)	16(16)	64(62)	1104(1008)	32(24)	64(60)
d_r (mm)	9.5	12.2	9.5	10.7	12.3	12.3	9.5	9.5	9.5
d_h (mm)	13	13	11	4	12	13	13	10	11
Axial power distribution	Chopped cosine	Chopped cosine	Chopped cosine	Chopped cosine	Uniform	Uniform/chopped cosine	Chopped cosine	Uniform	Uniform
ΔT_{sub}[K]	18/24	25–157	20/60	0.5–3	0[b]	9–12	0	5–35	46–118
p (MPa)	0.1/0.2	0.2–4.0	0.3/0.6	0.4	0.5/1.0	1.0–8.6	1.0/7.3/15.0	3.0/6.9/11.8	3.9–8.1
G (Kg m^{-2} s^{-1})	0.08	2.5–3.1	21–48[b]	42/91	833/1390	284–1988	2.2–84[b]	11–189	3.1–29
q[kW m^{-2}]	11	11/12	11–40	5/10	350–743[b]	225–3377[b]	5–45	9–170	11–74

[a] Light water high conversion reactor.
[b] Estimated values.

Table 2
Wide range void fraction correlations

Correlation	Year	Data Source	Avg ε	s
Zuber–Findlay	1965	Tube	−0.025	0.114
Ishii	1977	Tube	0 048	0.126
Gardner	1980	Tube	0.056	0.111
Liao, Parlos and Griffith	1985	Tube	0.028	0.094
Takeuchi	1992	Tube	0.040	0.083
Sun	1980	RB+Tube	−0.041	0.114
Jowitt	1981	RB	0.057	0.116
Sonnenburg	1989	RB+Tube	0.049	0.097
Toshiba	1989	RB	0.019	0.103
Dix	1971	RB	−0.010	0.092
Bestion	1985	RB+Tube	0.018	0.088
Chexal–Lellouche	1992	RB+Tube	−0.017	0.078
Inoue	1993	RB	−0.003	0.083
Maier and Coddington (1996)	1996	RB	−0.002	0.071

RB, Rod bundle.

$$\bar{\varepsilon} = \frac{1}{n}\sum_{i=1}^{n}\varepsilon_i, \tag{3}$$

$$s = \sqrt{\frac{\sum_{i=1}^{n}(\varepsilon_i - \bar{\varepsilon})^2}{n-1}}. \tag{4}$$

All correlations with a mean absolute error of more than 0.10 or with a standard deviation of more than 0.15 were discarded. The remaining 13 correlations can be loosely termed as 'wide range void fraction correlations' (see Table 2). Included in the final set of 13 correlations are four (five including the original Zuber and Findlay (1965)) which were developed from tube data. The remaining correlations are either specific to rod bundles or include rod bundle options. All of these 13 correlations except the one from Gardner (1980) are based upon the drift-flux model of Zuber and Findlay, so that the differences between these correlations are in the evaluation of the distribution and drift velocity parameter, C_0 and v_{gj}, respectively. These extend from constant values (Toshiba, 1989) obtained from a fit to experimental data and near constant values based upon physical considerations (Zuber and Findlay, 1965), to values with physical variable dependencies, particularly that of pressure. This can be included either directly (Sun et al., 1980) or by the inclusion of the vapor density (Dix, 1971; Jowitt, 1981; Bestion, 1985). Some of the correlations (Ishii, 1977; Liao et al., 1985; Sonnenburg, 1989; Takeuchi et al., 1992; Chexal et al., 1992) include an interdependence of C_0 and v_{gj}, thereby increasing the complexity of the solution and making their use in system codes more difficult without giving a dramatic increase in the quality of predictions. Finally, the correlation of Inoue et al. (1993) and a new correlation given in this paper (Maier and Coddington, 1997) calculate the pressure and mass flux dependency of C_0 and v_{gj} based on a fit to a wide range of experimental data.

The Zuber–Findlay correlation is treated separately, since it forms the foundation of most of the other correlations, while the other 12 correlations are divided into three groups. The first group consists of correlations derived from tube void fraction data. The correlations in the second group have a large value of the distribution parameter C_0, thus preventing predictions close to 1, as does the Zuber–Findlay correlation (see Section 3.1). The third group contains correlations which yield a good prediction over the whole range of void fractions. Also included in Table 2 is a correlation developed from the experimental data presented in this paper (Maier and Coddington, 1997).

3.1. Zuber–Findlay drift-flux correlation (Zuber and Findlay, 1965)

Although (Zuber and Findlay, 1965) also included models for the slug and annular flow regimes, it has to be noted that for the results presented in this paper only the drift velocity expression for churn-turbulent bubbly flow was used. Fig. 2 shows that no void fractions above 0.8 could be predicted. This is due to the constant value for the distribution parameter of 1.2, which limits the void fraction prediction with Eq. (1) to a maximum value of 0.83. In the original model, this region ($\alpha \geq 0.8$) was included in the annular flow regime where $C_0 = 1$. Fig. 2 also shows that the Zuber–Findlay correlation overpredicts data at low pressures: the mean error (from Eq. (2)) for the 81 data points with pressures below 1 MPa and measured void fractions below 0.8 is -0.122.

3.2. Correlations derived from tube void fraction data

The following four correlations by Ishii (1977), Gardner (1980), Liao et al. (1985) and Takeuchi et al. (1992) were derived from tube void fraction data.

3.2.1. Drift-flux model by Ishii (1977)

Flow regime dependent expressions for C_0 and v_{gj} were derived taking into account the interfacial geometry, the body-force field, shear stresses and the interfacial momentum transfer. Transition criteria (see Appendix A) between different flow regimes were developed based on the relative motion between phases. Since C_0 and v_{gj} are functions of the void fraction, the predictions are calculated iteratively. The Ishii model has considerable trouble predicting experimental void fractions at low pressures ($P < 1$ MPa) and high mass fluxes ($G > 100$ kg m^{-2} s^{-1}). These data points (BWR 4×4) are clearly underpredicted (23 data points with mean error 0.256). Data at high pressure (> 10 MPa) is also underpredicted (34 with 0.117 mean error). Additionally, Fig. 3 shows that despite the inclusion of annular, annular mist and liquid dispersed flow regime models, void fractions above 0.9 cannot be predicted.

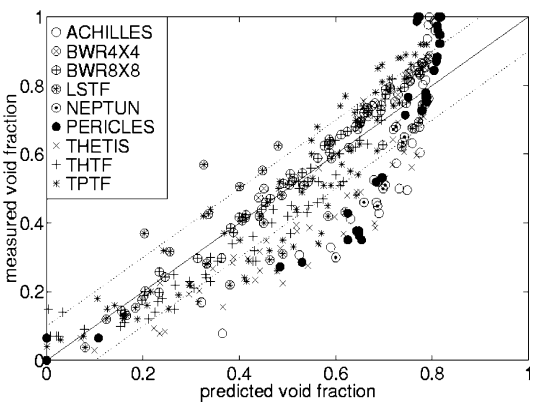

Fig. 2. Zuber–Findlay correlation void fraction predictions.

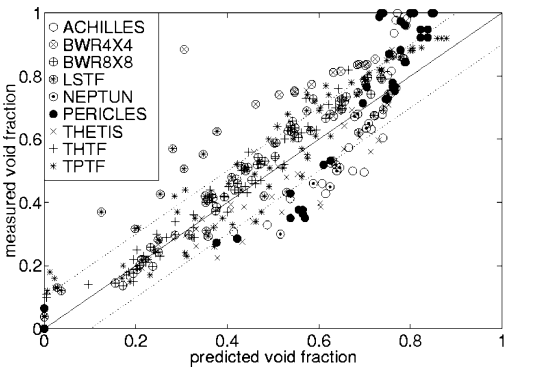

Fig. 3. Ishii model void fraction predictions.

3.2.2. Gardner correlation (Gardner, 1980)

This is the only correlation not based on the drift-flux approach. The void fraction is expressed as a function of the Froude number and a fitting constant, $m = 0.3$, and a dimensionless physical properties parameter, $K = 11.2$ (see Appendix A). Fig. 4 shows that experimental data from the BWR facilities is underpredicted for void fractions below 0.5 (20 data points with mean error 0.202) and overpredicted for higher void fractions (51 data points with mean error -0.129). An analysis of the data at pressures above 10 MPa indicates a tendency towards underprediction at high pressures (34 with mean error 0.139).

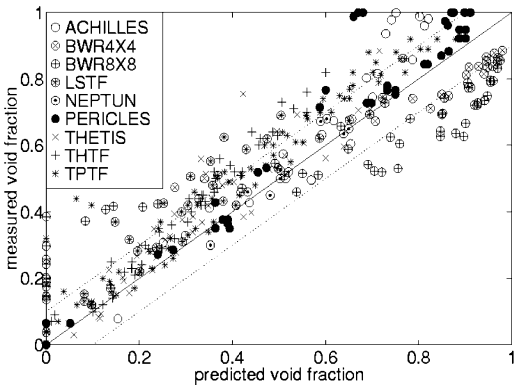

Fig. 4. Gardner correlation void fraction predictions.

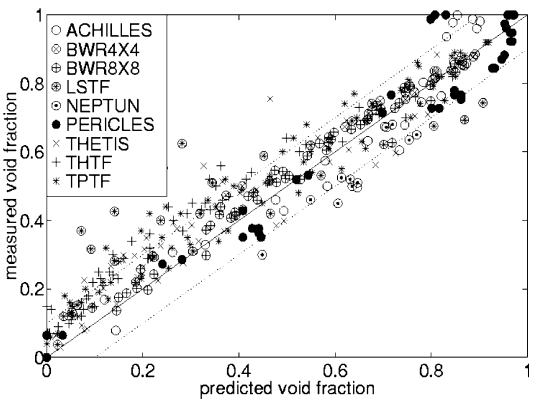

Fig. 6. Takeuchi correlation void fraction predictions.

3.2.3. Liao, Parlos and Griffith model (Liao et al., 1985)

The drift-flux model by Liao, Parlos and Griffith (Liao et al., 1985) is based primarily on the Ishii model with the addition of a separate expression for the drift velocity in the bubbly flow regime. These changes lead to a smaller scatter of the data points. For example, this correlation shows in Fig. 5 a lower standard deviation, 0.094, when compared to that for the Ishii model, 0.126 (see Fig. 3). Data at low pressures ($P < 1$ MPa) and low mass fluxes ($G < 10$ kg m^{-2} s^{-1}) is generally underpredicted by the correlation (51 data points with mean error 0.143).

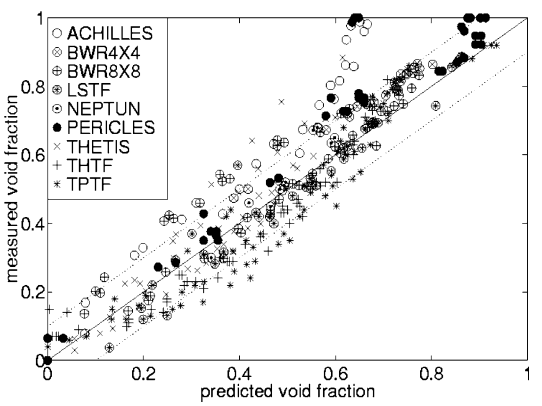

Fig. 5. Liao et al. model void fraction predictions.

3.2.4. Takeuchi et al. correlation (Takeuchi et al., 1992)

The Takeuchi correlation was developed on the basis of experimental data from a 1/100-scale steam generator test-facility (small diameter tubes), and is based on a generalized form of the flooding correlation by Wallis (1969). Fig. 6 shows an underprediction of data for experimental void fractions below 0.35 (108 data points with mean error 0.062). Again, for high pressure (> 10 MPa) experiments the void fractions are underpredicted (34 data points with mean error 0.149).

3.3. Correlations including rod bundle data with large values of C_0

The four correlations presented below have all relatively large values of the distribution parameter C_0 for the pressure range of the experiments analyzed. For instance, C_0 is 1.08 for the Toshiba correlation (Morooka et al., 1989), 1.12 for the Jowitt et al., (1984) correlation and 1.19 for the correlation by Sonnenburg (1989). The minimal value of 1.06 for the Sun correlation only occurs for experimental data at 15 MPa, for experiments at or below 10 MPa the smallest value yielded by this correlation is C_0 is 1.11.

3.3.1. Sun void fraction correlation (1980)

The Sun correlation (Sun et al., 1980) is a modification of the Zuber–Findlay model. A pressure dependency is introduced in the distribu-

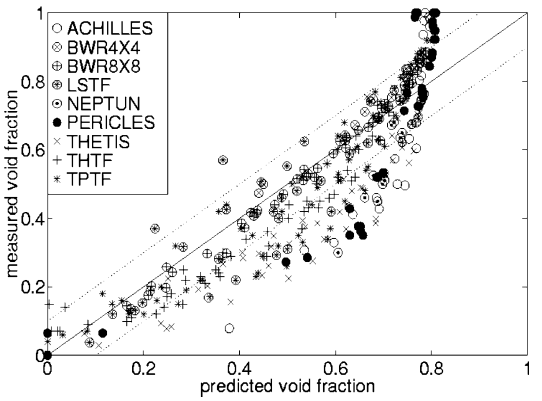

Fig. 7. Sun correlation void fraction predictions.

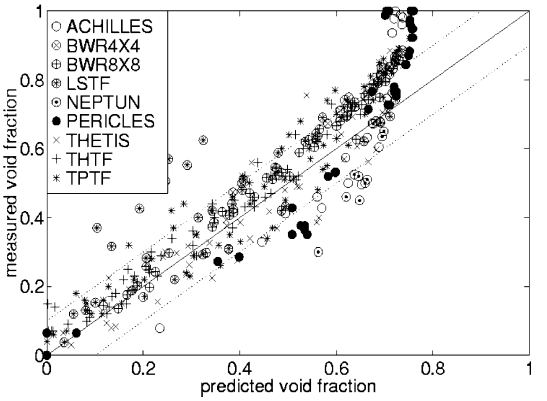

Fig. 9. Sonnenburg model void fraction predictions.

tion parameter C_0 and a different constant factor is used for the drift velocity calculation v_{gj}. As can be seen from Table 2 and by comparing Fig. 7 to Fig. 2 the differences with the Zuber–Findlay correlation predictions are minimal.

3.3.2. Jowitt correlation (1981)

The Jowitt correlation (Jowitt et al., 1984) was derived from a series of experiments at pressures ranging from 0.2–4 MPa, a similar range to the THETIS experiments analyzed here. The empirical expressions for C_0 and v_{gj} are strongly dependent on system pressure through the pressure dependency of the gas density. Fig. 8 shows a systematic trend towards underprediction with increasing void fraction, so that while the Jowitt correlation is acceptable for low void fractions, it underpredicts almost all experimental data with void fractions above 0.6 (84 data points with mean error 0.131).

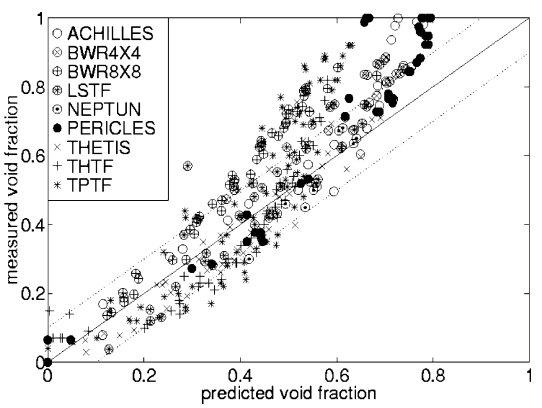

Fig. 8. Jowitt correlation void fraction predictions.

3.3.3. Drift-flux model by Sonnenburg (1989)

Sonnenburg combined the flooding correlation by Wallis (1969) and the drift-flux model by Ishii (1977) to obtain a new full-range drift-flux model. In this approach, the drift velocity is a function of the void fraction and the predictions are then calculated iteratively. In Table 2 it can be seen that the main advantage of the Sonnenburg model over the Zuber and Findlay correlation is the reduction of the standard deviation of the predictions. By comparing Fig. 9 to Fig. 2, this effect can be seen as a smaller spread of the data points and a better prediction for data at pressures below 1 MPa.

3.3.4. Toshiba correlation (1989)

For this correlation (Morooka et al., 1989) constant values for C_0 and v_{gj} were obtained from a least squares fit to the data from the BWR 4×4 experiments.

Correspondingly, the prediction of the experiments used for the development of the correlation (BWR 4×4) is excellent (20 data points with mean error < 0.001). As can be seen in Fig. 10 the value of 1.08 for the distribution parameter C_0, which is lower than for the Zuber–Findlay correlation, enables void fraction predictions up to 0.91. The prediction quality is quite good with

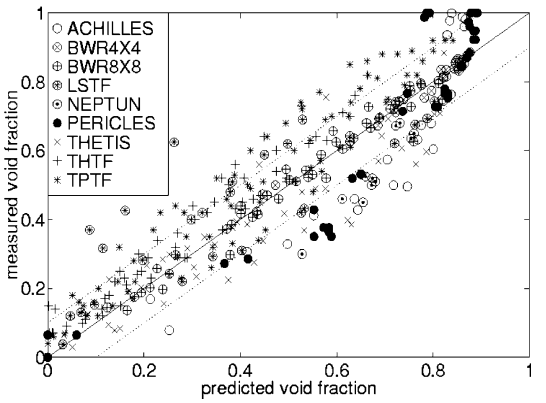

Fig. 10. Toshiba correlation void fraction predictions.

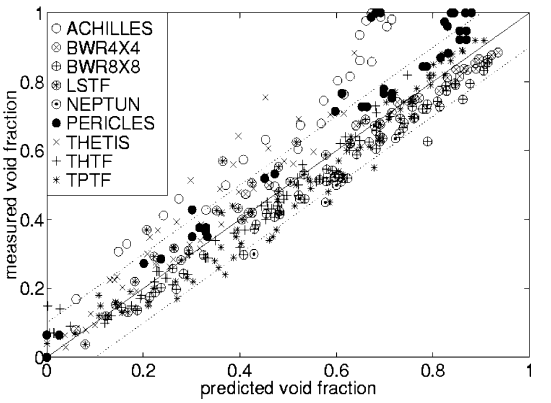

Fig. 12. Bestion correlation void fraction predictions.

the exception of data at pressures above 10 MPa, for which the void fractions are underpredicted (34 data points with mean error 0.166).

3.4. Correlations derived from rod bundle data providing good predictions over the whole range of void fractions

3.4.1. Dix Model (1971)

The Dix model (Chexal et al., 1986) was derived for the analysis of BWRs under operating conditions. The drift velocity is that of the Zuber–Findlay correlation with a different constant factor. A dependency on pressure and superficial velocities is introduced for the distribution parameter C_0. The results of this analysis (Fig. 11) show that the Dix correlation can also be applied to PWR test facilities. Discrepancies occur for experiments at high pressures ($P > 10$ MPa) where the data is underpredicted (34 data points with mean error 0.110), and at both low pressures and low mass fluxes ($P < 1$ MPa; $G < 10$ kg m^{-2} s^{-1}) where the void fraction is overpredicted (51 with -0.106 mean error).

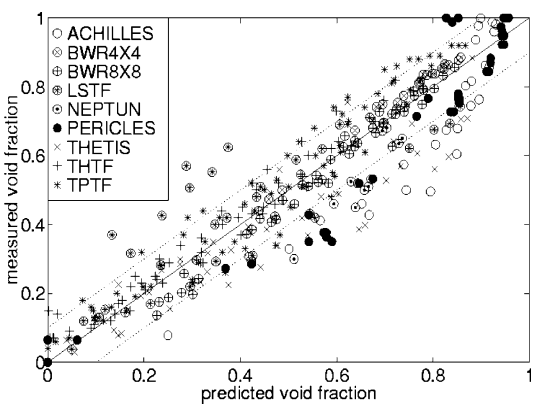

Fig. 11. Dix model void fraction predictions.

3.4.2. Bestion drift-flux correlation (1985)

Developed for use in the thermal hydraulic code CATHARE, this correlation (Bestion, 1990) has a geometry dependent (on hydraulic diameter) drift velocity expressions. For the present analysis the expression for rod bundles was used. Due to the absence of a value for the distribution parameter C_0 in the reference available to the authors a value of 1 was used to span the whole range of void fractions. A parametric study showed that other values of C_0 lead to a decrease of the overall prediction quality.

Despite the simplicity of this correlation, it yields very good results for most of the experimental data analyzed. Fig. 12 shows that the only experiments where the predicted void fractions are not satisfactory are at both low pressures and low mass fluxes ($P < 1$ MPa; $G < 10$ kg m^{-2} s^{-1}), where the data is underpredicted (51 data points with mean error 0.149).

3.4.3. Chexal–Lellouche drift-flux correlation (Chexal et al., 1992)

The Chexal-Lellouche drift-flux correlation (Chexal et al., 1992) is based on the drift-flux

theory by Zuber and Findlay and uses basically the same expression for the drift velocity. It was developed to cover not only the full range of pressures, mass fluxes and void fractions, but also for different fluid types (steam–water, air–water, hydrocarbons, etc.) and flow angles. It has been qualified against several sets of experimental data from test facilities with geometries typical of BWR and PWR fuel assemblies and from pipe test sections with various diameters.

Fig. 13 shows that the prediction quality is excellent apart from several data points from THETIS experiments. This is due to the fact that these experiments were transient boil-down experiments, while the calculations in this paper assumed a steady state configuration. Additionally, a slight underprediction tendency can be determined for data at pressures above 10 MPa (34 data points with mean error 0.057).

3.4.4. Void correlation by Inoue et al. (1993)

This correlation, also based on the Zuber–Findlay drift-flux model, was derived from Japanese void fraction data from the BWR 8×8 facility. An evaluation of the effects of the major variables provided the selection criteria for the parameters to be used in the expressions for the distribution factor and the drift velocity. These variables were mass flow rate W (kg s^{-1}) and pressure P (MPa). Polynomial expressions were

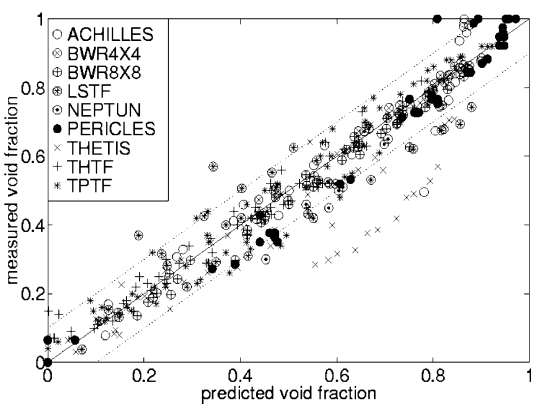

Fig. 13. Chexal–Lellouche correlation void fraction predictions.

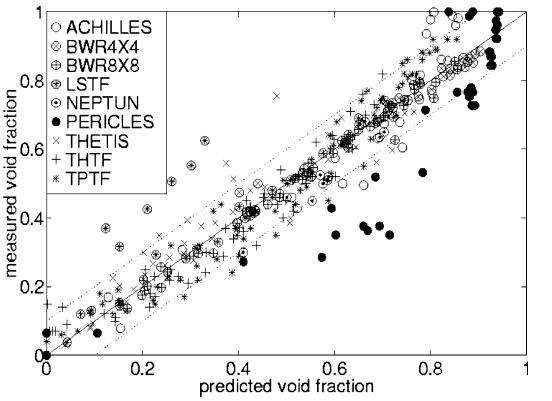

Fig. 14. Inoue correlation void fraction predictions.

then developed for the drift velocity and the distribution parameter. With the exception of high pressure data ($P > 10$ MPa), where the experimental data is slightly underpredicted (34 data points with mean error 0.069) and data from the PERICLES facility, which is slightly overpredicted (47 with mean error -0.065), the predictions are excellent for the whole range of conditions covered in the experimental data base (see Fig. 14).

3.4.5. Maier and Coddington correlation (Maier and Coddington, 1997)

The void fraction predictions with this correlation are better than for the other correlations (see Table 2). This is due to the fact that it was obtained by a least squares fit to all of the experimental data. It shows clearly that a purely empirical approach to the evaluation of C_0 and v_{gj} of the drift-flux equation by Zuber and Findlay (1965) leads to very good results.

Fig. 15 shows that this correlation also has a small tendency towards overprediction for data at pressures higher than 10 MPa (34 data points with mean error 0.035).

3.5. Comparison of the performance of the correlations

Table 2 shows the numerical values computed by using Eq. (1) and Eq. (3) in order to assess the performance of the different correlations studied

in this paper. The best correlations, i.e. those with the lowest average error and standard deviation are the ones developed for rod bundles (RB), which is to be expected as the experimental data base covers PWR and BWR rod bundle data. The table also shows that complex correlations like Chexal–Lellouche, or others requiring iterative solutions, produce no significant improvement in mean error or standard deviation compared to the more direct correlations of Bestion, Inoue and Maier and Coddington for the wide range of conditions covered by the data base used for the work reported in this paper.

4. Assessment of the Chexal–Lellouche drift-flux model as implemented in the system code RETRAN-3D

The models and correlations reviewed in Section 3, and others used by thermal-hydraulic analysis codes to predict void fraction distribution were developed from, and validated against, steady-state experimental data, due to the limited availability of transient data. It is important, however, to be able to assess the ability of these models to predict transient vapor formation and transport along heated channels, since these codes are often applied to the analysis of transient scenarios. Section 4.1 presents the results and analysis of the assessment of the Chexal–Lellouche drift-flux model as implemented in the system code RETRAN-3D (Paulsen et al., 1996), against data from transient boiling experiments carried out by the Japanese Nuclear Power Engineering Corporation (NUPEC) (Hori et al., 1993, 1994, 1995, 1996) in a nuclear fuel assembly subchannel.

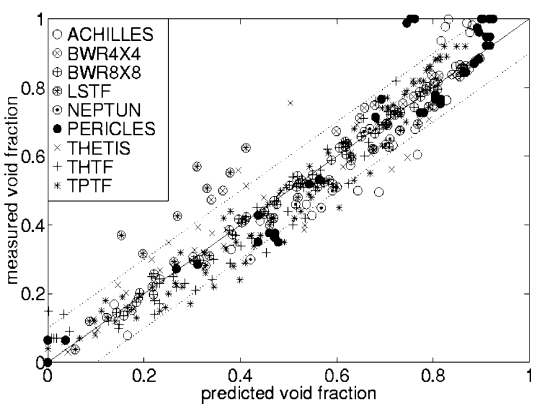

Fig. 15. Maier and Coddington correlation void fraction predictions.

4.1. The implementation of the Chexal–Lellouche drift-flux models in RETRAN-3D

The implementation of the Chexal–Lellouche correlation in the system code RETRAN-3D calculates the drift velocity, v_{gj}, and distribution parameter, C_0, and Eq. (1) is used to calculate a slip velocity, V_{SL}, defined as $v_{liquid} - v_{steam}$ from the values of C_0, and v_{gj}. The slip velocity is then incorporated into the basic mixture momentum and energy conservation equations. The solution of these equations together with the conservation of mass and the appropriate boiling models for vapor production determine the transport of mass and energy and the thermal-hydraulic conditions along the system. Based on these conditions, the void fraction is then calculated. This approach is typical of system codes that use the drift-flux approach for two-phase flow.

Two slip models are available in RETRAN-3D. They both add a fourth equation to the three basic conservation equations. In the first, the fourth equation is an algebraic expression that relates V_{SL} to C_0 and v_{gj}, and in the second, an additional momentum equation for V_{SL} which makes use of the parameters C_0 and v_{gj} to determine the liquid vapor interfacial friction is used.

4.2. Description of the experimental conditions

The experimental rig consisted of a pressure vessel, a flow channel and a simulated subchannel heated by Inconel 600 skin heaters. These produced a uniform axial power distribution and had a heated length of 1.5 m. Void fraction data was measured by using γ-ray computer tomography (CT) scanner and γ-densitometers to produce transient and steady-state averaged void fractions. Both measurement systems were stationed at the same location near the top of the test section.

Table 3
Sub channel analysis transients

Transient	Pressure (MPa)	Inlet temperature (°C)	Inlet mass flux (kg m^{-2})	Heat flux (MW m^{-2})
Pressure	15.5 (-0.03 MPa s^{-1})	315	12	1.23
Inlet temperature	15.5	305 ($+1$ °C s^{-1})	12	1.70
Inlet mass flux 15%	15.5	315	12 (-15% s^{-1})	1.23
Inlet mass flux 25%	15.5	315	12 (-25% s^{-1})	1.23

Table 3 displays the four different subchannel transients analyzed. For each transient, the linear rate of variation of the modified system variable is written within brackets next to its initial value. However, the assessment calculations were carried out by using the actual variation of the system variables given in (Hori et al., 1994). All the experiments were performed at 15.5 MPa and under simulated conditions relevant to PWR ATWS.

4.3. Computer model

The RETRAN-3D computer model of the experimental rig consisted of one-dimensional control volumes. Care was taken to place the center of the volumes at which the void fraction data was computed coincidental with the experimental measuring stations.

The transient calculations were initiated following a steady state solution that set the computer model conditions to the same values as those measured in the experiments. After the transients were initiated, the appropriate system variables were modified according to the data provided in Hori et al. (1994). Fig. 16 displays a schematic view of the RETRAN-3D subchannel model.

The slip was calculated based on the Chexal–Lellouche drift-flux model using both the algebraic formula and the momentum equation for the slip velocity. In addition, calculations were made with the slip velocity equal to one, i.e. both phases flowing at the same speed, which represents a homogeneous flow.

4.4. Mass flow rate transients

Two mass flow rate transients were analyzed. The first one with a 15% s^{-1} flow reduction rate, and the second one with a flow reduction rate of 25% s^{-1}. In both cases, the mass flow rate was increased after reaching a minimum value to prevent the burn-out of the heater rods. In Figs. 17 and 18, the increase and subsequent decrease of the measured void fraction follows closely the variation in the inlet mass flow rate, reaching a maximum at about the same time when the inlet mass flow rate reached a minimum. Both slip

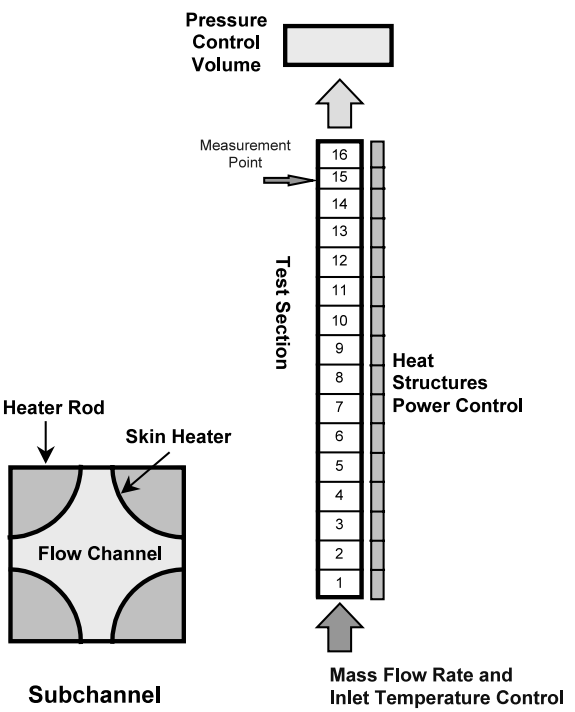

Fig. 16. Schematic of the RETRAN-3D computer model for the subchannel analysis.

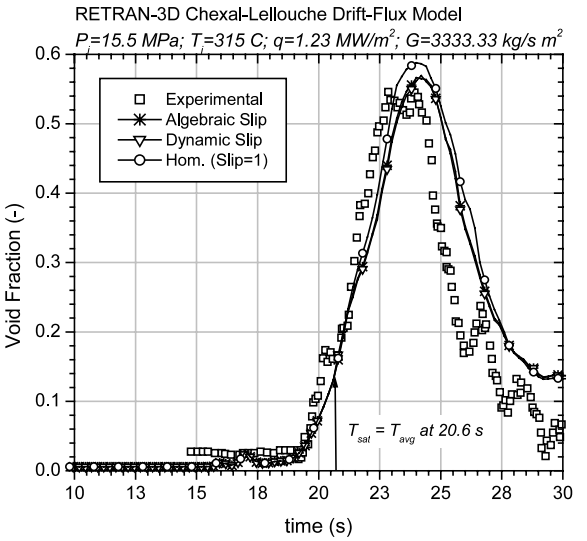

Fig. 17. Subchannel flow transient. Mass flow decrease -15% s^{-1}.

models, using the Chexal–Lellouche correlation, were able to model this behavior well, although the increasing-flow part of the transient presented the largest discrepancies.

It is important to note that both slip models predicted correctly the time for the start of the void fraction rise, and an acceptable time for the

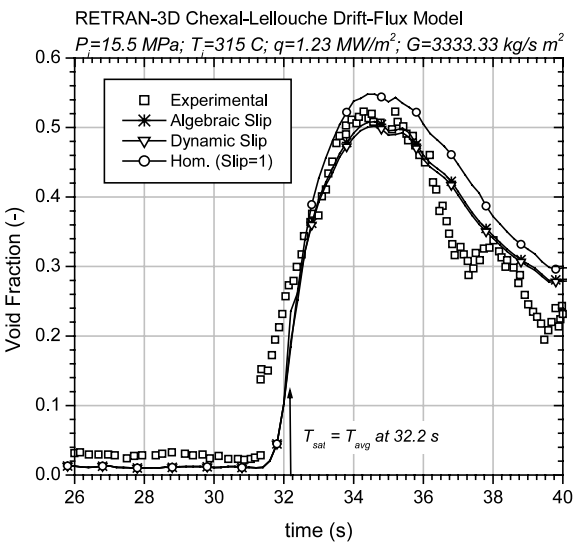

Fig. 18. Subchannel flow transient. Mass flow decrease -25% s^{-1}.

void peak value. This indicates a good performance of void fraction formation models (not addressed in this paper) and vapor transport under the very rapid varying conditions of both transients.

The second phase of the transients, when the inlet mass flow rate was increased after reaching a minimum, appears in the figures as a decrease in the measured and calculated void fractions. The discrepancy observed between the code results and the experimental data during this phase can be attributed to the probable condensation of part of the vapor in the lower subcooled boiling region as the injection of subcooled liquid was rapidly increased (in ~ 2 s). This could explain the rapid 'collapse' of void fraction and the subsequent 'oscillatory' increase. The physical process appears to be that the increase in the subcooled liquid inlet flow sweeps away the superheated boundary layer containing the emerging wall vapor bubbles, condensing them and overcooling the heater walls, so suppressing (temporarily) subcooled boiling. Subcooled boiling is then re-established, at the new flow rate, some time later. This 'transient condensation' behaviour is of course not captured by the steady-state models contained in the codes.

4.5. Pressure transient

The reduction of the system pressure decreased the saturation enthalpy, and for a constant inlet mass flow rate and subcooling, the vapor production increased as the pressure decreased. Fig. 19 shows that both slip models used to calculate the phase relative velocities followed closely the experimental data up to the point in time at which the conditions at the measuring station became saturated (~ 66.6 s). After this time, the void production below the measuring point increased substantially with the region of saturated boiling moving downwards with decreasing system pressure. The predictions by the two slip models departed gradually from the experimental data.

The assumption of equal phase velocity substantially improved the results, to the point that the differences between the predicted, and the measured void fraction fell within the experimen-

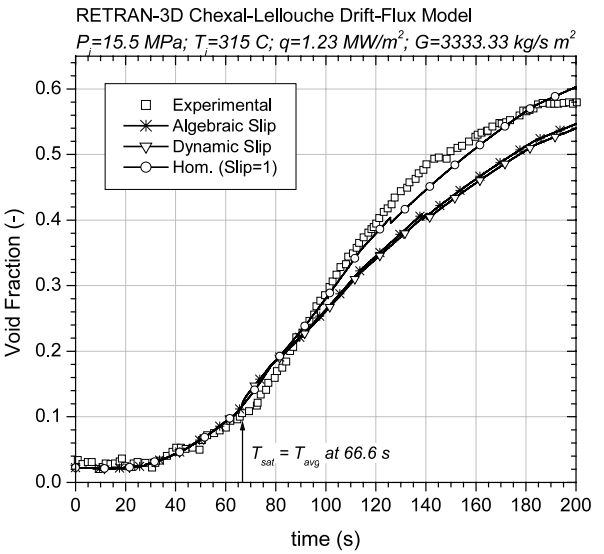

Fig. 19. Subchannel flow transient. Pressure decrease -0.03 MPa s^{-1}.

tal accuracy of about 6%, for most of the transient. This result shows clearly the dominant effect of the slip ratio on the resultant void fraction for a relatively slow transient.

4.6. Inlet temperature transient

The temperature transient reduced the inlet subcooling by increasing the inlet temperature by 1 °C s^{-1}. Thus, for a constant inlet mass flow rate and system pressure, vapor production was increased in the subchannel.

According to Fig. 20, the results of both slip models using the Chexal–Lellouche correlation followed a similar trend to that discussed for the pressure transient, yielding large discrepancies as the transient progressed. In this case, though, the void fraction during the initial subcooled boiling dominated phase of the transient and the rising void fraction slope were very well predicted, with the calculated void fraction becoming lower than the measured value as the subchannel went into saturate boiling.

Similar to the pressure transient analyzed above, the use of a slip ratio equal to 1.0 improved significantly the prediction of void fraction, particularly during the later stage of the transient when the majority of the test section experienced saturated boiling conditions.

5. Summary

5.1. Assessment of void fraction correlations

From the resulting numerical evaluation of the various correlations we observe the following:

1. Surprisingly, two of the tube based correlations, namely Liao et al. (1985) and Takeuchi et al. (1992) produce standard deviations which are as low as the best of the rod bundle correlations.
2. The high values of C_0 in the correlations by Sun et al. (1980), Jowitt (1981), Sonnenburg (1989) and Toshiba (1989) limit the prediction of high void fraction data, as they cannot predict annular flow where C_0 should be close to unity.
3. The standard deviation of the 'best' five correlations lies between 0.071 and 0.092 with a mean absolute error of 0.002 to 0.018. Surprisingly one of these five is the rather old correlation by Dix from 1971. The remaining four include two correlations currently used in sys-

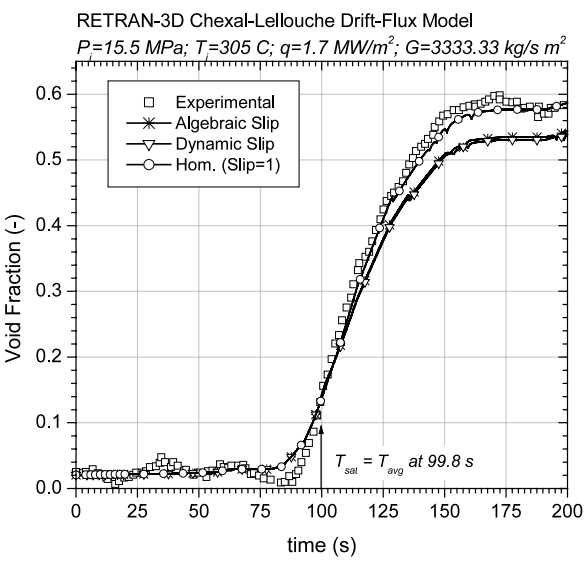

Fig. 20. Subchannel flow transient. Temperature increase 1 °C s^{-1}.

tem analysis codes i.e. Chexal–Lellouche Chexal et al. (1992) (RELAP5, RETRAN-3D) and Bestion (1985) (CATHARE). The final two are those of Inoue and Maier and Coddington, where the functional dependence of C_0 and v_{gj} was obtained from a fit to experimental data.

4. As stated above, complex correlations like Chexal et al. (1992), or others requiring iterative solutions produce no significant improvement in mean error or standard deviation compared to the more direct correlations of Bestion, Inoue and Maier and Coddington.
5. Most of the correlations had difficulty predicting one or more of the experimental data sets. For example the THETIS experiments proved difficult for some correlations because of the low (almost zero) inlet flows, while other correlations had difficulty in general predicting low pressure low flow data sets. The only systematic trend detected was the underprediction of the high pressure data from TPTF and particularly LSTF.

5.2. Subchannel transient experiments

The assessment has shown that acceptably good predictions of transient void fraction distribution along heated channels are possible with models originally developed primarily from steady state conditions. The comparisons with experimental data are good for transients in which system conditions vary relatively slowly and, therefore, could be considered as 'quasi-steady state'. But the conclusion is also valid in the case of relatively fast transients (i.e. substantial variations of system parameters in a few seconds). The one area in which this is not the case is when the inlet subcooled liquid flow rate is increased and transient over-cooling and condensation of the wall voids occurs. During this phase, when condensation (driven by subcooled water injection) can be expected, transient effects are observed which are clearly outside the scope of the code models.

For pressure conditions typical of PWR normal operation (15 MPa) there is a tendency to underestimate the saturated void fraction due to the overprediction of the slip ratio, especially for relatively slow transients (pressure and temperature), when a good prediction of the vapor transport along the heated channel is important to obtain an accurate transient void fraction distribution. For fast transients the effect of the lack of accuracy in predicting the slip ratio appears to be of less significance, since the void fraction distribution seems to be more dependent on the boiling models (subcooled and saturated) in the code. This is in general agreement with the analysis of the steady-state experiments reported in Coddington et al., (1999). The under prediction of the slip ratio was compensated for in the RETRAN-3D analysis by setting the slip ratio to 1.0 ($V_{SL} = 0.0$), thus forcing both phases to flow at the same speed. A clear improvement in the void fraction prediction in saturated boiling conditions was then observed, which agrees with many experimental observations reported elsewhere regarding vapor formation and transport along heated channels at high pressures. In such cases, both phases appear to flow at approximately the same speed along the channel.

Finally, the results discussed above suggest that the interpretation of void fraction distribution at high pressures, should be made with caution in transient or steady state calculations when the slip ratio predicted by a code (whether from correlations, as for example in RETRAN-3D, or by solving the vapor and liquid momentum equations) is significantly different from one, in particular for relatively slow transients.

6. Conclusions

In this paper we reviewed and assessed the ability of a range of drift-flux correlations to predict rod bundle void fraction data for conditions typical of those in a nuclear reactor core. One of these correlations was then used in the context of a system analysis code to analyze transient sub-channel void fraction experiments. The results of this work show the validity and usefulness of the relatively simple approach of the drift-flux model for this type of analysis.

Acknowledgements

The authors wish to thank Nuclear Electric of the UK for providing access to the ACHILLES data and Daniel Maier for his help in performing the calculations. This work was partly funded by the Swiss Federal Nuclear Safety Inspectorate (HSK) and the Swiss Federal Office of Energy (BFE).

Appendix A. Expressions of the correlations

Zuber and Findlay (1965)

$$C_0 = 1.2, \quad v_{gj} = 1.53\left(\frac{g\sigma\Delta\rho}{\rho_l^2}\right)^{1/4}.$$

Drift-flux model by Ishii (1977)

For churn turbulent flow:

$$C_0 = \left(1.2 - 0.2\sqrt{\frac{\rho_g}{\rho_l}}(1 - \exp(-18\alpha))\right),$$

$$v_{gj} = (C_0 - 1)j + \sqrt{2}\left(\frac{g\sigma\Delta\rho}{\rho_l^2}\right)^{1/4}$$

For annular flow

$$C_0 = 1 + \frac{1-\alpha}{\alpha + \sqrt{((1 + 75\,(1-\alpha))/\sqrt{\alpha})\,(\rho_g/\rho_l)}},$$

$$v_{gj} = (C_0 - 1)\left[j + \sqrt{\frac{gd_h\Delta\rho\,(1-\alpha)}{0.015\rho_l}}\right].$$

The criteria for flow regime transition is given by

$$|j_g| \le \sqrt{\frac{gd_h\Delta\rho}{\rho_g}}\left(\frac{1}{C_0} - 0.1\right)$$

for churn turbulent flow.

Gardner correlation (1980)

$$\frac{\alpha}{\sqrt{1-\alpha}} = K[F_D P^m]^{2/3}$$

with $K = 11.2$, $m = 0.3$,

$$F_D = \frac{\sqrt{\rho_l}j_g}{(\Delta\rho g\sigma)^{1/4}} \quad \text{and} \quad P = \frac{\rho_g v_l^2\sqrt{\Delta\rho g}}{\sigma^{3/2}}.$$

Liao, Parlos and Griffith model (Liao et al., 1985) For bubbly flow,

$$j_l > 2.34 - 1.07\left(\frac{g\sigma\Delta\rho}{\rho_l^2}\right)^{1/4},$$

then

$$C_0 = 1, \quad v_{gj} = 1.53(1-\alpha)^2\left(\frac{g\sigma\Delta\rho}{\rho_l^2}\right)^{1/4},$$

For churn turbulent flow

$$C_0 = \left(1.2 - 0.2\sqrt{\frac{\rho_g}{\rho_l}}(1 - \exp(-18\alpha))\right),$$

$$v_{gj} = 0.33\left(\frac{g\sigma\Delta\rho}{\rho_g^2}\right)^{1/4}$$

For annular flow,

$$|j_g| > \sqrt{\frac{gd_h\Delta\rho}{\rho_g}}\left(\frac{1}{C_0} - 0.1\right)$$

then

$$C_0 = 1 + \frac{1-\alpha}{\alpha + 4\sqrt{\rho_g/\rho_l}},$$

$$v_{gj} = (C_0 - 1)\sqrt{\frac{gd_h\Delta\rho(1-\alpha)}{0.015\rho_l}}.$$

Drift-Flux Correlation by Takeuchi et al. (1992)

$$C_0 = 1.11775 + 0.45881\alpha - 0.57656\ \alpha^2,$$

$$v_{gj} = k\frac{C_0(1 - C_0\alpha)}{m^2 + C_0\alpha(\sqrt{\rho_g/\rho_l} - m^2)}\sqrt{\frac{gd_h\Delta\rho}{\rho_l}}$$

where

$$k = \sqrt{\frac{K_{D^*}^2}{D^*}}, \quad m = 1.367,$$

the Kutateladze number

$$K_{D^*} = \sqrt{D^* \cdot \min\left(\frac{1}{2.4}, \frac{10.24}{D^*}\right)}$$

and

$$D^* = d_h\sqrt{\frac{g\Delta\rho}{\sigma}}.$$

Void fraction correlation by Sun et al. (1980)

$$C_0 = \frac{1}{0.82 + 0.18(p/p_{crit})},$$

$$v_{gj} = 1.41\left(\frac{g\sigma\Delta\rho}{\rho_l^2}\right)^{1/4}$$

Jowitt correlation (Jowitt, 1981)

$$C_0 = 1 + 0.796\ \exp\left(-0.061\sqrt{\frac{\rho_l}{\rho_g}}\right),$$

$$v_{gj} = 0.034\left(\sqrt{\frac{\rho_l}{\rho_g}} - 1\right).$$

Drift-flux model by Sonnenburg (1989)

$$C_0 = 1 + \left(0.32 - 0.32\sqrt{\frac{\rho_g}{\rho_l}}\right),$$

$$v_{gj} = \frac{C_0(1 - C_0\alpha)}{(C_0\alpha/\sqrt{gd_h\Delta\rho/\rho_g}) + (1 - C_0\alpha/\sqrt{gd_h\Delta\rho/\rho_l})}.$$

Toshiba correlation (1989)

$$C_0 = 1.08, \quad v_{gj} = 0.45.$$

Dix model (1971)

$$C_0 = \frac{j_g}{j}\left(1 + \left(\frac{j}{j_g} - 1\right)^{(\rho_g/\rho_l)^{0.1}}\right),$$

$$v_{gj} = 2.9\left(\frac{g\sigma\Delta\rho}{\rho_l^2}\right)^{1/4}.$$

Bestion drift-flux correlation (Bestion, 1985)

$$C_0 = 1, \quad v_{gj} = 0.188\sqrt{\frac{gd_h\Delta\rho}{\rho_g}}.$$

Chexal–Lellouche drift-flux correlation (Chexal et al., 1992)

$$C_0 = \frac{L}{K_0 + (1 - K_0)\alpha^r},$$

$$v_{gj} = 1.41\left(\frac{g\sigma\Delta\rho}{\rho_l^2}\right)^{1/4} C_2C_3C_4C_9,$$

with

$$L = \frac{1 - \exp(-C_1\alpha)}{1 - \exp(-C_1)}, \quad C_1 = \frac{4p_{crit}^2}{p(p_{crit} - p)},$$

$$K_0 = B_1 + (1 - B_1)\left(\frac{\rho_g}{\rho_l}\right)^{1/4}, \quad r = \frac{1.0 + 1.57\rho_g/\rho_l}{1 - B_1},$$

and

$$B_1 = \min\left(0.8, \frac{1}{1 + \exp(-\mathrm{Re}/60\,000)}\right),$$

$$\mathrm{Re} = \max(\mathrm{Re}_l, \mathrm{Re}_g),$$

The constants in the drift velocity are computed as

$$C_2 = \begin{cases} 0.4757\left(\ln\left(\frac{\rho_l}{\rho_g}\right)\right)^{0.7} & \text{if } \frac{\rho_l}{\rho_g} \le 18 \\ \begin{cases} 1 & \text{if } C_5 \ge 1 \\ \left(1 - \exp\left(\frac{-C_5}{1 - C_5}\right)\right)^{-1} & \text{if } C_5 < 1 \end{cases} & \text{if } \frac{\rho_l}{\rho_g} > 18 \end{cases},$$

$$C_3 = \max\left(0.5, 2\exp\left(\frac{-|\mathrm{Re}_l|}{60\,000}\right)\right),$$

$$C_4 \begin{cases} 1 & \text{if } C_7 \ge 1 \\ \left(1 - \exp\left(\frac{-C_7}{1 - C_7}\right)\right)^{-1} & \text{if } C_7 < 1 \end{cases},$$

$$C_5 = \sqrt{150\frac{\rho_g}{\rho_l}}, \quad C_7 = \left(\frac{0.09144}{d_h}\right)^{0.6}, \quad \text{and}$$

$$C_9 = (1 - \alpha)^{B_1}$$

Void correlation by Inoue et al. (1993)

$$C_0 = 6.76 \times 10^{-3}p + 1.026$$

$$v_{gj} = (5.10 \times 10^{-3}W + 6.91 \times 10^{-2}) \times (9.42 \times 10^{-2}p^2 - 1.99p + 12.6)$$

Maier and Coddington correlation (Maier and Coddington, 1997)

$$C_0 = C_1{\cdot}p + C_2,$$

$$v_{gj} = (v_1{\cdot}p^2 + v_2{\cdot}p + v_3){\cdot}G + (v_4{\cdot}p^2 + v_5{\cdot}p + v_6)$$

$$C_1 = 2.57 \times 10^{-3} \quad C_2 = 1.0062$$

$$v_1 = 6.73 \times 10^{-7} \quad v_4 = 5.63 \times 10^{-3}$$

$$v_2 = -8.81 \times 10^{-5} \quad v_5 = -1.23 \times 10^{-1}$$

$$v_3 = 1.05 \times 10^{-3} \quad v_6 = 8.00 \times 10^{-1}$$

Appendix B. Nomenclature

C_0	Distribution parameter
g	Gravitational acceleration [m s^{-2}]
j	Superficial velocity [m s^{-1}]
n	Number of data points
s	Standard deviation
v_{gj}	Drift velocity [m s^{-1}]
P_i	Inlet pressure [MPa]
T_i	Inlet temperature [°C]
T_{sat}	Saturation temperature [°C]
d_h	Hydraulic diameter [m]
p	Pressure [MPa]
W	Mass flow [kg s^{-1}]
Greek letters	
α	Void fraction
ε	Absolute error
ρ	Density [kg m^{-3}]
$\Delta\rho$	$\rho_l - \rho_g$ [kg m^{-3}]
σ	surface tension [N m^{-1}]
Subscripts	
g	Gas phase
l	Liquid phase

References

Anklam, T.M., Miller, R.F., 1982. Void fraction under high pressure, low flow conditions in rod bundle geometry. Nucl. Eng. Des. 75, 99–105.

Anoda, Y., Kukita, Y., Tasaka, K., 1990. Void fraction distribution in rod bundle under high pressure conditions, Proc., ASME Winter Annual Meeting, Advances in Gas-Liquid Flows, pp. 283–289.

Bestion, D., 1990. The physical closure laws in the CATHARE code. Nucl. Eng. Des. 124, 229–245.

Chexal, B., Horowitz, J., Lellouche, G., 1986. An assessment of eight void fraction models for vertical flows, NSAC-107, Electric Power Research Institute, Nuclear Safety Analysis Center, Palo Alto.

Chexal, B., Lellouche, G., Horowitz, J., Healzer, J., 1992. A void fraction correlation for generalized applications. Prog. Nucl. Ener. 27 (4), 255–295.

Coddington, P., Aounallah, Y., Maier, D., Reehda, D., 1999. Assessment of the subcooled boiling models in RETRAN-3D and TRAC-BF1 against rod bundle and subchannel data, Proceedings of NURETH-9.

Deruaz, R., Clement, P., Veteau, J.M., 1985. Study of two-dimensional effects in the core of a light water reactor during the ECC's phase following a loss of coolant accident, EUR 10076 EN, Commissariat a l'Energie Atomique, Centre d'Etude Nucleaires de Grenoble, Service des Transferts Thermiques, Grenoble.

Dreier, J., Analytis, G., Chawla, R., 1988. NEPTUN-III reflooding and boil-off experiments with an LWHCR fuel bundle simulator: experimental results and initial code assessment efforts. Nucl. Tech. 80, 93–106.

Gardner, G.C., 1980. Fractional vapour content of a liquid pool through which vapour is bubbled. Int. J. Multiphase Flow 6, 399–410.

Hori, K., Akiyama, Y., Miyazaki, K., Kurosu, T., Sugiyama, S., 1994. Transient void fraction measurement in a single channel simulating one channel for a PWR fuel assembly, Proc. of the 10th Nuclear Thermal-hydraulics ANS Winter Meeting, pp. 56–68.

Hori, K., Akiyama, Y., Miyazaki, K., Kurosu, T., Sugiyama, S., 1995. Void fraction in a single channel simulating one subchannel of a PWR fuel assembly, Proc. of the 1st International Symposium on Two-Phase Flow Modeling and Experimentation.

Hori, K., Akiyama, Y., Miyazaki, K., Nishioka, H., Takeda, N., 1996. Total evaluation of in bundle void fraction measurement test of PWR fuel assembly. Proc. of ICONE-4 1 (Part B), 801–811.

Hori, K., Miyazaki, K., Kurosu, T., Sugiyama, S., Matsumoto, J., Akiyama, Y., 1993. In bundle void fraction measurement of PWR fuel assembly. Proc. of ICONE-2 1, 69–76.

Inoue, A., Kurosu, T., Yagi, M., Morooka, S., Hoshide, A., Ishizuka, T., Yoshimura, K., 1993. In-bundle void measurement of a BWR fuel assembly by an X-ray CT scanner: assessment of BWR design void correlation and development of new void correlation, Proc. of the ASME/JSME Nuclear Engineering Conference, 1, pp. 39–45.

Ishii, M., 1977. One-dimensional drift-flux model and constitutive equations for relative motion between phases in various two-phase flow regimes, ANL-77-47, Argonne National Laboratory, Argonne.

Jowitt, D., Cooper, C.A., Pearson, K.G., 1984. The THETIS 80% blocked cluster experiment, Part 5: level swell experiments, AEEW-R 1767, AEEE Winfrith, Safety and Engineering Science Division, Winfrith UK.

Kumamaru, H., Kondo, M., Murata, H., Kukita, Y., 1994. Void-fraction distribution under high-pressure boil-off conditions in rod bundle geometry. Nucl. Eng. Des. 150, 95–105.

Liao, L.H., Parlos, A., Griffith, P., 1985. Heat tranfer, carry-over and fall back in PWR steam generators during transients, NUREG/CR-4376, EPRI NP-4298.

Maier, D. and Coddington, P., 1997. Review of wide range void correlations against and extensive data base of rod bundle void measurements, Proc. of ICONE-5, Paper No. 2434.

Maier, D., Coddington, P., 1996. Validation of RETRAN-03 against a wide range of rod bundle void fraction data. ANS Transactions 75, 372–374.

Mitsutake, T., Morooka, S., Suzuki, K., Tsunoyama, S., Yoshimura, K., 1990. Void fraction estimation within rod bundles based on three-fluid model and comparison with X-ray CT void data. Nucl. Eng. Des. 120, 203–212.

Morooka, S., Inoue, A., Oishi, M., Aoki, T., Nagaoka, K., Yoshida, H., 1991. In-Bundle void measurement of BWR fuel assembly by X-ray CT scanner, Proc. of ICONE-1, Paper 38, pp. 237–243.

Morooka, S., Ishizuka, T., Iizuka, M., Yoshimura, K., 1989. Experimental study on void fraction in a simulated BWR fuel assembly (evaluation of cross-sectional averaged void fraction). Nucl. Eng. Des. 114, 91–98.

Paulsen, M., et al., 1996. RETRAN-3D a program for transient thermal-hydraulic analysis of complex fluid systems, Vol. 1, Theory and Numerics, EPRI Report NP-7450.

Pearson, K.G., and Denham, M.K., 1989. Achilles un-ballooned cluster experiments, Part 4: low pressure level swell experiments, AEEW-R 2339, United Kingdom Atomic Energy Authority, Winfrith Technology Centre, Safety and Engineering Science Division, Winfrith UK.

Sonnenburg, H.G., 1989. Full-range drift-flux model base on the combination of drift-flux theory with envelope theory. Proc. of NURETH-4 2, 1003–1009.

Sun, K.H., Duffey, R.B., and Peng, C.M., 1980. A thermal-hydraulic analysis of core uncovery, Proc. of the 19th National heat transfer conference, experimental and analytical modeling of LWR safety experiments, pp. 1–10.

Takeuchi, K., Young, M.Y., Hochreiter, L.E., 1992. Generalized drift flux correlation for vertical flow. Nucl. Sc. Eng. 112, 170–180.

Wallis, G.B., 1969. One-Dimensional Two-phase Flow. McGraw-Hill Book Company, New York, USA.

Zuber, N., Findlay, J.A., 1965. average volumetric concentration in two-phase flow systems. J. Heat Transfer 87, 453–468.